

Surface waves with photorefractive nonlinearity

T. H. Zhang, X. K. Ren, B. H. Wang, C. B. Lou, Z. J. Hu, W. W. Shao, Y. H. Xu, H. Z. Kang, J. Yang, D. P. Yang, L. Feng, and J. J. Xu

Photonics Research Center, The MOE Key Lab of Advanced Technique and Fabrication for Weak-Light Nonlinear Photonics Materials, and Tianjin Key Lab of Photonics Materials and Technology for Information Science, Nankai University, 300071 Tianjin, People's Republic of China

(Received 15 January 2007; published 24 July 2007)

The photorefractive surface waves with photorefractive nonlinearity of diffusion, drift, and photovoltaic effect is studied numerically for the first time. We find out that the essential cause of photorefractive surface waves is diffusion mechanism, but not drift and photovoltaic effects. The photovoltaic effect only has strong influence on the profile of photorefractive surface waves; the applied external electric field can also change the profile of the surface waves, and even destroy the mode upon a threshold, which provides a possible method to transform the modes of surface waves between high-frequency modes and low-frequency modes.

DOI: [10.1103/PhysRevA.76.013827](https://doi.org/10.1103/PhysRevA.76.013827)

PACS number(s): 42.65.Jx, 42.65.Hw

I. INTRODUCTION

The photorefractive effect is a phenomenon in which the local index of refraction of a medium is changed by the illumination of a beam of light with spatial variation of the intensity [1]. It is generally due to a combination of various physical mechanisms such as photoinduced charge generation, charge carrier transport, and the electro-optic effect. The photorefractive effect has two unique characteristics. First, the optical response of the photorefractive effect is generally independent of intensity. This unusual property allows many applications to be realized using low power. The second unique characteristic is the nonlocal nature of the refractive index grating, which is the origin of optical beam coupling in the photorefractive crystal (PRC). Due to these unique characteristics, the photorefractive effect has direct applicability to photonics, including optical image processing, parallel optical logic, pattern recognition, and phase conjugation.

In 1992 and 1994, Daisy and Fischer studied the nonlinear behavior of light waves at an interface between linear and nonlinear (Kerr or photorefractive) media [2,3]. In 1995, a new type of surface wave (SW), namely, photorefractive surface wave (PR SW) was suggested by Garcia Quirino *et al.* [4]. Generally speaking, these PR SWs can propagate along the boundary of the PRC with a metal, a dielectric, or other photorefractive crystals.

The most attractive feature of the PR SW is that the concentration of beam energy in the narrow surface layer significantly increases the operation speed of the photorefractive devices without the need for specially prefabricated waveguiding structures [5]. A very strong enhancement of all nonlinear surface optical phenomena, such as surface absorbed molecular luminescence, Raman scattering, surface second harmonic generation (SHG), etc., may be expected due to PR SW excitation. A giant enhancement of surface SHG excited by the PR SW has been observed at the surface of the BaTiO₃ and Sr_{0.6}Ba_{0.4}NbO₃(SBN:60) crystals [6,7]. That may be considered as an example of the guiding of light with light in a self-induced surface waveguide, which may find application in such emerging soliton related techniques as writing virtual photonic circuits [8].

There are three transport mechanisms in the photorefractive effect: diffusion, drift, and photovoltaic effect, all of which can contribute to the PR SW. PR SW with a diffusion mechanism of nonlinearity has been analyzed theoretically [4,9] and observed experimentally in BaTiO₃, [10,11]. PR SW with diffusion and drift nonlinearity was studied in 1997 for the first time [12]. In 2001, Aleshkevich *et al.* studied the formation and stability of localized surface waves [13]. In 2004, Alvarado-Méndez *et al.* studied the spatial soliton on the boundary of nonlinear media under diffusion-drift nonlinearity [14]. They demonstrated that the diffusion mechanism causes a self-bending effect on the soliton, and in consequence it is launched to nonlinear interface. PR SW at the interface between air and the SBN crystal with drift and diffusion nonlinearity has been observed experimentally in 2005 [15,16]. The influence of the photovoltaic effect on PR SW has been studied neither theoretically nor experimentally.

The photorefractive surface waves with photorefractive nonlinearity of diffusion, drift, and photovoltaic effect is studied numerically. We find out that the essential cause of the PR SW is diffusion mechanism, but not drift and photovoltaic effects. The photovoltaic effect has strong influence on the profile of the PR SW; the applied external electric field can also change the profile of the PR SW, and even destroy the mode upon a threshold, which provides a possible method to transform the modes of surface waves between high-frequency modes and low-frequency modes.

II. THEORETICAL MODEL

We consider a slit laser beam (transverse extent of the beam along the y axis greatly exceeds that along the x axis) propagating in the direction of the z axis at the interface of the PRC and another medium. The left half-space ($x < 0$) is occupied by an ideal metal or a linear dielectric with the refractive index n' , while the right half-space ($x > 0$) is occupied by the PRC, which is taken here to be LiNbO₃ with its optical c axis oriented along the x axis.

The electric-field component $E(x, z)$ of the surface waves satisfies the wave equation

$$\nabla^2 E(x, z) + k^2 E(x, z) = 0, \quad (1)$$

where $k = k_0[n + \Delta n(x)]$, $k_0 = 2\pi/\lambda_0$, λ_0 is the wavelength in vacuum; n is the undisturbed refractive index of the PRC; $\Delta n(x)$ is the nonlinear refractive index change of the PRC, which corresponds to $[n + \Delta n(x)]^2 = n^2 - n^4 r_{\text{eff}} E_{\text{sc}}(x)$ for photorefractive nonlinearity; r_{eff} is the effective electro-optical coefficient; $E_{\text{sc}}(x)$ is the induced space-charge field. We look for the stationary solution as $E(x, z) = A(x) \exp(i\beta z) = A'(x) I_d^{1/2} \exp(i\beta z)$, where β is the propagating constant of surface wave, $A'(x)$ is the normalized real amplitude of the PR SW, and I_d is the dark intensity of the PRC.

In turn, the induced space-charge field E_{sc} can be obtained from the band transport equations, which describe the PR effect in a medium. Considering the short-circuit circumstance, in one dimension and steady state these equations are

$$s[I(x) + I_d](N_D - N_D^+) = \gamma_R N_D^+ N, \quad (2)$$

$$J(x) = q\mu N E_{\text{sc}}(x) + k_B T \mu \frac{dN}{dx} - \kappa \alpha I(x), \quad (3)$$

$$\frac{\partial J(x)}{\partial x} = 0 \quad \text{or} \quad J(x) = \text{const}, \quad (4)$$

where N_D^+ and N_D are the ionized donor density and the donor density, respectively; N_A is the acceptor density, N is the electron density, $I(x)$ is the light intensity of the PR SW along x , J is the current density, s is the photoexcitation cross section, γ_R is the carrier recombination rate, μ and q are the electron mobility and the charge, respectively, k_B is Boltzmann's constant, T is the absolute temperature, κ is the Glass constant, and α is the absorption coefficient.

We can use a method similar to that in Ref. [17] to simplify Eqs. (2)–(4) by keeping in mind that the following approximations hold true in a typical PRC: $N_D^+ \gg N$, $N_A \gg N$, and $N_D^+ \approx N_A$. In this case Eq. (2) yields the following result:

$$N = \frac{s(N_D - N_A)[I(x) + I_d]}{\gamma_R N_A}. \quad (5)$$

At this point let us also assume that the light density $I(x)$ attains a constant value at $x \rightarrow \infty$; that is, $I(x \rightarrow \infty) = I_\infty$. In this region Eqs. (2)–(4) require that the space-charge field be independent of x ; i.e., $E_{\text{sc}}(x \rightarrow \infty) = E_0$, where E_0 is the external electric field. Therefore from Eq. (5) the electron density N in the region ($x \rightarrow \infty$), denoted by N_0 , can be subsequently determined and is given by

$$N_0 = s(N_D - N_A)(I_\infty + I_d) / (\gamma_R N_A). \quad (6)$$

From Eqs. (3) and (6), the current density $J(x)$ in the region ($x \rightarrow \infty$) can be given by

$$J_\infty = q\mu N_0 \left(E_0 - E_P \frac{I_\infty}{I_\infty + I_d} \right), \quad (7)$$

where $J_\infty = J(x \rightarrow \infty)$ and $E_P = \kappa \alpha \gamma_R N_A / [\mu q s (N_D - N_A)]$.

In the region of $I(x)$ varying with x , from Eqs. (2) and (3), we have

$$J(x) = q\mu N \left[E_{\text{sc}} + \frac{k_B T dN}{qN dx} - E_P \frac{I(x)}{I(x) + I_d} \right]. \quad (8)$$

Equation (4) implies that the current density $J(x)$ is constant everywhere; that is, $J(x) = J_\infty$. Therefore from Eqs. (7) and (8) we have

$$N_0 \left(E_0 - E_P \frac{I_\infty}{I_\infty + I_d} \right) = N \left[E_{\text{sc}}(x) + \frac{k_B T dN}{qN dx} - E_P \frac{I(x)}{I(x) + I_d} \right]. \quad (9)$$

In turn, the space-charge field E_{sc} can be obtained from Eq. (9) as follows:

$$E_{\text{sc}}(x) = E_0 \frac{I_\infty + I_d}{I(x) + I_d} - \frac{k_B T}{q} \frac{1}{I(x) + I_d} \frac{dI}{dx} + E_P \frac{I(x) - I_\infty}{I(x) + I_d}. \quad (10)$$

The envelope evolution equation inside the PRC can now be established by inserting $[n + \Delta n(x)]^2 = n^2 - n^4 r_{\text{eff}} E_{\text{sc}}(x)$ and Eq. (10) into Eq. (1) with I'_∞ according to $I'_\infty = |A'(x \rightarrow \infty)|^2 = I_\infty / I_d$ as follows:

$$\begin{aligned} \frac{d^2 A'(x)}{dx^2} + \gamma \frac{A'^2(x)}{A'^2(x) + 1} \frac{dA'(x)}{dx} - a \frac{(I'_\infty + 1)A'(x)}{A'^2(x) + 1} \\ - b \frac{[A'^2(x) - I'_\infty]A'(x)}{A'^2(x) + 1} + cA'(x) = 0, \quad x \geq 0, \end{aligned} \quad (11)$$

where $\gamma = 2k_0^2 n^4 r_{\text{eff}} k_B T / q$, $a = k_0^2 n^4 r_{\text{eff}} E_0$, $b = k_0^2 n^4 r_{\text{eff}} E_P$, and $c = k_0^2 n^2 - \beta^2$.

The envelope equation inside dielectric is

$$\frac{d^2 A'(x)}{dx^2} - (\beta^2 - k_0^2 n^4) A'(x) = 0, \quad x < 0. \quad (12)$$

The first term of Eq. (11) describes the diffraction spreading of the light beam. The second, third, and fourth terms describe the influence of diffusion, drift, and photovoltaic effect of the photorefractive nonlinearity, respectively. The sign of a depends on the direction of the applied external electric field E_0 .

In the case when the left half-space is occupied by an ideal metal, inside the PRC we have an equation with boundary conditions as follows:

$$\begin{aligned} \frac{d^2 A'(x)}{dx^2} + \gamma \frac{A'^2(x)}{A'^2(x) + 1} \frac{dA'(x)}{dx} - a \frac{(I'_\infty + 1)A'(x)}{A'^2(x) + 1} \\ - b \frac{[A'^2(x) - I'_\infty]A'(x)}{A'^2(x) + 1} + cA'(x) = 0, \\ A'(0) = 0, \quad \frac{dA'(0)}{dx} = B, \end{aligned} \quad (13)$$

where B is an arbitrary constant.

For a steady surface wave at the interface of the PRC-dielectric, $A(x)$ always shows asymptotic behavior in $x < 0$ regions as

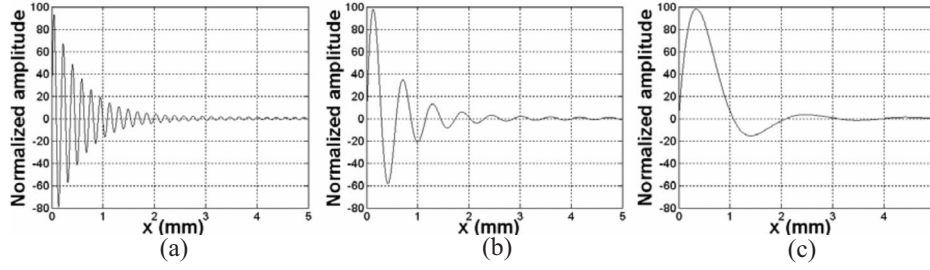


FIG. 1. Profile of the PR SW modes with a diffusion mechanism: (a) $c=k_0^2n^2-\beta^2=1.21\times 10^9\text{ m}^{-2}$; (b) $c=1.21\times 10^8\text{ m}^{-2}$; (c) $c=1.21\times 10^7\text{ m}^{-2}$.

$$A'(x) = B \exp(\sqrt{\beta^2 - k_0^2 n'^2} x), \quad x < 0, \quad A'(-\infty) = 0. \quad (14)$$

Taking into account the continuity of the electric field on the interface, we obtain

$$\begin{aligned} \frac{d^2 A'(x)}{dx^2} + \gamma \frac{A'^2(x)}{A'^2(x) + 1} \frac{dA'(x)}{dx} - a \frac{(I'_\infty + 1)A'(x)}{A'^2(x) + 1} \\ - b \frac{[A'^2(x) - I'_\infty]A'(x)}{A'^2(x) + 1} + cA'(x) = 0, \quad A'(0) = B, \\ \frac{dA'(0)}{dx} = B\sqrt{\beta^2 - k_0^2 n'^2}, \quad x > 0. \end{aligned} \quad (15)$$

Equation (11) is a typical damped oscillation equation, so we advance an oscillator model, by which the profile of the PR SW $A'(x)$ can be treated as the damped oscillation of an oscillator with two external forces. Under this model, the second term, the third term, the fourth term, and the fifth term of Eq. (11) can be treated as the damping, the external force corresponding to an applied external electric field, the external force corresponding to the photovoltaic effect, and the restoring force, respectively. The two external forces and the restoring force constitute effective restoring force F , which is related to E_0 , E_p , and β . From Eq. (11) effective restoring force F and spatial frequency $K(x)$, which varies along x can be described as

$$F = a \frac{(I'_\infty + 1)A'(x)}{A'^2(x) + 1} + b \frac{[A'^2(x) - I'_\infty]A'(x)}{A'^2(x) + 1} - cA'(x), \quad (16)$$

$$K(x) = \sqrt{c - a \frac{(I'_\infty + 1)}{A'^2(x) + 1} - b \frac{A'^2(x) - I'_\infty}{A'^2(x) + 1} - \frac{\gamma^2 A'^4(x)}{4[A'^2(x) + 1]^2}}. \quad (17)$$

Without the diffusion mechanism of photorefractive nonlinearity ($\gamma=0$), the PR SW will always oscillate without decay, just as the oscillations of an oscillator without damping. So diffusion mechanism is necessary to the formation of the PR SW, that is to say, it is the diffusion mechanism that lets the profile of the PR SW decay from surface to the volume and ensures efficient concentration of light power in a narrow layer near the surface. The photovoltaic effect and

external electric field are not essential causes, which only have strong influences on the PR SW induced by the diffusion mechanism.

III. MODES OF THE PHOTOREFRACTIVE SURFACE WAVES

Considering the case without photovoltaic effect and external electric field ($a=0$, $b=0$), diffusion is the dominant mechanism of nonlinearity and Eq. (11) can be simplified as

$$\frac{d^2 A'(x)}{dx^2} + \gamma \frac{A'^2(x)}{A'^2(x) + 1} \frac{dA'(x)}{dx} + cA'(x) = 0. \quad (18)$$

We all know that the guided modes in a slab waveguide are discrete and each discrete mode is determined by the propagation constant β , which is corresponding to the incident angle. Just like the modes in a slab waveguide, each mode of the PR SW is also determined by the corresponding propagation constant β , which is related to the incident angle. But the modes of the PR SWs have continuous character.

Equation (18) has no analytical solutions. We study the modes of the SWs at the interface of the PRC and ideal metal numerically using the Runge-Kutta method. The material parameters used in the numerical calculation are $n=2.2$, $r_{\text{eff}}=30.9\times 10^{-12}\text{ m/V}$, and $T=300\text{ K}$ [15]. Figure 1(a) shows the mode available for the case of a comparatively small propagation constant. Figure 1(c) shows the mode available for the case of a comparatively large propagation constant. One can see from Fig. 1 that the spatial frequency decreases with the increasing of propagation constant β . We call the modes with high spatial frequency as high-frequency modes, such as the mode in Fig. 1(a), while the modes with low spatial frequency are called low-frequency modes, such as the mode in Fig. 1(c).

From Fig. 1 we also know that the propagation constant of low-frequency modes is always very large, which corresponds to the case of grazing incidence. For a crystal of small size, grazing incidence cannot be realized easily; consequently low-frequency modes can be hardly excited. Contrary to low-frequency modes, high-frequency modes can be obtained and controlled comparatively easily. From Eqs. (17), we can find that spatial frequency $K(x)$ of the PR SW can be adjusted by photovoltaic effect and applied external electric field. That provides a possibility to transform the PR

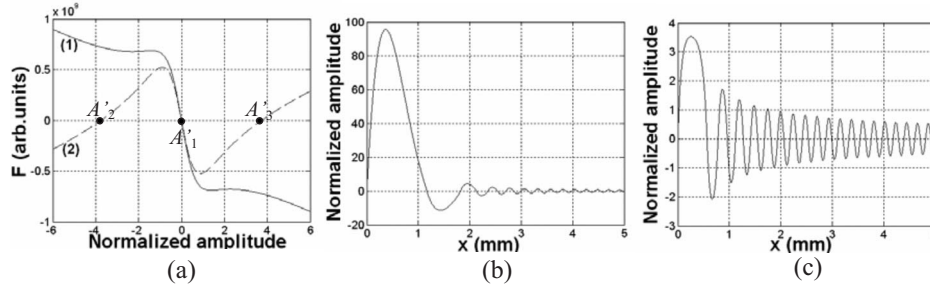


FIG. 2. (a) Effective restoring force F as a function of the normalized amplitude $A'(x)$: curves (1) and (2) correspond to $b=1.20 \times 10^9 \text{ m}^{-2}$ and $b=1.23 \times 10^9 \text{ m}^{-2}$, respectively, when $c=1.21 \times 10^9 \text{ m}^{-2}$. [(b) and (c)] Profiles of the modes corresponding to curves (1) and (2) in (a), respectively.

SW between high-frequency modes and low-frequency modes.

IV. INFLUENCE OF PHOTOVOLTAIC EFFECT

When a beam is incident on the boundary of a photovoltaic crystal such as LiNbO_3 , the influence of photovoltaic effect has to be considered. In this case, effective restoring force F can be described as

$$F = b \frac{A'^2(x) - I'_\infty}{A'^2(x) + 1} A'(x) - cA'(x). \quad (19)$$

For a practical PR SW, the amplitude of damped oscillation should converge gradually to zero from surface to volume, and be balanced at an equilibrium position corresponding to $F=0$, i.e., under the zero value of the effective restoring force, $A'(x \rightarrow \infty)$ will no longer oscillate. If $I'_\infty = |A'(x \rightarrow \infty)|^2 \neq 0$, we can find from Eq. (19) that $F=cA'(x \rightarrow \infty) \neq 0$ and $A'(x)$ will oscillate continuously. So we can draw a conclusion that $I'_\infty = |A'(x \rightarrow \infty)|^2 = 0$.

We analyze the influence of the photovoltaic effect on the PR SW numerically using LiNbO_3 as a sample; and the material parameters are $N_A=3.3 \times 10^{18} \text{ cm}^{-3}$, $N_D=6.6 \times 10^{18} \text{ cm}^{-3}$, $s=6.2 \times 10^{-1} \text{ cm}^2/\text{J}$, $\gamma_R=1.0 \times 10^{-9} \text{ cm}^3/\text{s}$, $\mu=0.1 \text{ cm}^2/\text{V s}$, and $\alpha=0.55 \text{ cm}^{-1}$ [18].

We consider two cases: the case $b < c$ and the case $b > c$.

A. For the case of $b < c$

When $b < c$, the effective restoring force as a function of $A'(x)$ is shown as curve (1) in Fig. 2(a) and the corresponding mode of the PR SW is shown in Fig. 2(b). We can see from curve (1) that there is only one intersection of F and $A'(x)$ at $A'_1=0$. We can also see from curve (1) that F always exhibits an attractive force around $A'_1=0$: if $A(x) > 0$, $F < 0$; whereas if $A(x) < 0$, $F > 0$. That is to say, F always tends to return the oscillator to this position. So $A'_1=0$ is a steady equilibrium position, and the oscillating can converge at 0. Compared to Fig. 1(a), which is induced by diffusion mechanism only, one can see from Fig. 2(b) that the spatial frequency becomes low, especially the front half part of the PR SW. One can see from Eqs. (16) and (17) that the photovoltaic effect acts as an external force and can reduce the restore force and results in the reduction of $K(x)$; moreover, the

influence of the photovoltaic effect on $K(x)$ depends on the amplitude $A'(x)$; the larger $A'(x)$ is, the stronger the change of $K(x)$ is. So the photovoltaic effect mainly reduces the spatial frequency for the front half part of the PR SW with large $A'(x)$, while the change of spatial frequency for the back half part of the PR SW with small $A'(x)$ is slight, as shown in Fig. 2(b). The result indicates that the photovoltaic effect has a strong influence on the PR SW induced by the diffusion mechanism, which enables people to get low-frequency modes at comparatively small incident angles.

B. For the case of $b > c$

Curve (2) in Fig. 2(a) shows the effective restoring force when $b > c$ and Fig. 2(c) shows the mode of the PR SW corresponding to curve (2). We can see from curve (2) that there are three intersections of F and $A'(x)$: $A'_{1,2,3}$. Similar to the case of $b < c$, F always exhibits attractive force around $A'_1=0$, so A'_1 is an equilibrium position and the oscillating can converge at 0. Though the PR SW can exist steadily, we can see from Fig. 1(c) that the peak of the SW is very small. It indicates that the power of the PR SW is too low to have some applications. When the oscillator moves around A'_2 or A'_3 , F always exhibits as a repulsive force, i.e., F always tends to keep the oscillator away from this position. So A'_2 and A'_3 are not equilibrium positions, and the decaying oscillating cannot converge at the couple of nonzero values at $x \rightarrow \infty$.

V. INFLUENCE OF EXTERNAL ELECTRICAL FIELD

When an external electric field is applied to the photovoltaic crystal, effective restoring force F and spatial frequency $K(x)$ can be described by Eqs. (16) and (17). From the above analysis, we can know that the influence of the photovoltaic effect on the PR SW depends on the relation between b and c . So the influence of the external electrical field on the PR SW of the photovoltaic crystal should also be analyzed for two cases: $b < c$ and $b > c$.

A. For the case of $b < c$

We can use a method similar to that in Sec. IV and draw a similar conclusion that $F=0$ at $x \rightarrow \infty$. At $x \rightarrow \infty$, we can simplify Eq. (16) as $F=(a-c)A'(x)$ for $I'_\infty = |A'(x \rightarrow \infty)|^2$. The

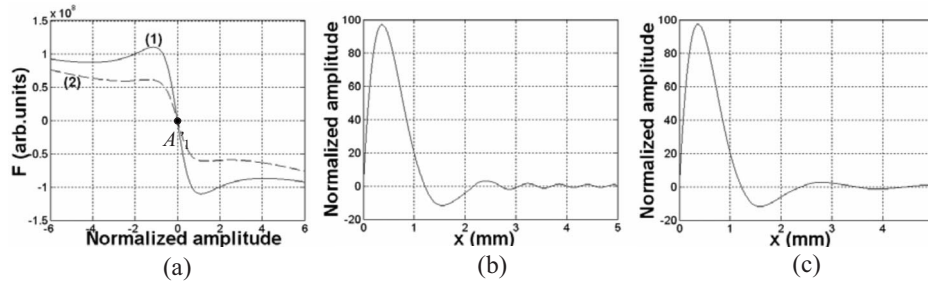


FIG. 3. (a) Effective restoring force F as a function of the normalized amplitude $A'(x)$: curves (1) and (2) correspond to $E_0 = 150$ V/cm and $E_0 = 170$ V/cm, respectively. [(b) and (c)] Profiles of the modes corresponding to $E_0 = 150$ V/cm and $E_0 = 170$ V/cm, respectively. The parameters b and c are $b = 1.20 \times 10^9$ m $^{-2}$, $c = 1.21 \times 10^9$ m $^{-2}$.

solution of $F=0$ should be $A'(x)=0$. So we can draw a conclusion that $I'_\infty = |A'(x \rightarrow \infty)|^2 = 0$. The curves (1) and (2) in Fig. 3(a) show effective restoring forces under applying the external electric field to the photovoltaic crystal; while Figs. 3(b) and 3(c) show the modes of the PR SW corresponding to curves (1) and (2), respectively.

Comparing Fig. 2(b) with Figs. 3(b) and 3(c), we can see that the spatial frequency of the mode will become lower when an external electric field is applied and the long oscillating tail will vanish when the electric field is high enough. The higher the external electric field is applied, the lower the spatial frequency becomes. One can see from Eqs. (16) and (17) that a positive applied external electric field acts as an external force and can reduce the restore force and results in the reduction of $K(x)$; the influence of an applied external electric field on $K(x)$ depends on the value of $A'(x)$ and E_0 . On one hand, $K(x)$ decreases with the increasing of E_0 . On the other hand, the smaller $A'(x)$ is, the stronger the change of $K(x)$ is; so the applied external electric field mainly reduces the spatial frequency for the back half part of the PR SW with small $A'(x)$, while the change of spatial frequency for the front half part of the PR SW with large $A'(x)$ is slight, as shown in Figs. 3(b) and 3(c). This provides a possibility to transform the PR SW from high-frequency modes to low-frequency modes by an external electric field.

From Fig. 3(a) we can see that there is only one intersection of F and $A'(x)$ at $A'_1 = 0$. When the oscillator moves around A'_1 , F always exhibits an attractive force around this equilibrium position. When a low external electric field $E_0 < (k_0^2 n^2 - \beta^2) / k_0^2 n^4 r_{\text{eff}}$ (i.e., $a < c$) is applied, $A'(x)$ exhibits a

decaying oscillation with a variable spatial frequency and converges at 0, as shown in Figs. 3(b) and 3(c). Moreover, continuously increasing E_0 , when a high external electric field $E_0 > (k_0^2 n^2 - \beta^2) / k_0^2 n^4 r_{\text{eff}}$ (i.e., $a > c$) is applied, there will be three intersections F and $A'(x)$: $A'_{1,2,3}$, as shown in Fig. 4(a). A'_1 is not an equilibrium position because F always exhibits as a repulsive force around this position, while $A'_{2,3}$ are two equilibrium positions because F always exhibits as an attractive force. As a result, $A'(x)$ does not converge at $A'_1 = 0$ but converges at the couple of nonzero values at $x \rightarrow \infty$. That will be contrary to the conclusion $I'_\infty = |A'(x \rightarrow \infty)|^2 = 0$ mentioned above. It indicates that there is no solution for $A'(x)$ when a high external electrical field is applied to the photovoltaic crystal.

From the above analysis, we can draw a conclusion that the applied external electrical field has a threshold as $E_{\text{th}} = (k_0^2 n^2 - \beta^2) / k_0^2 n^4 r_{\text{eff}}$, above which the PR SW will be destroyed and cannot exist steadily. For a certain material E_{th} is mainly determined by propagation constant β . The modes with high β will be more sensitive to the applied external electrical field. Figures 3(b) and 3(c), and Figs. 4(b) and 4(c) show the influence of the applied external electric field E_0 within the range of 0.15–1 kV/cm on the surface waves of the photovoltaic crystal. From Fig. 4(b) we can see that $A(x)$ converges at a nonzero value when $E_0 = 0.2$ kV/cm and the mode has been destroyed.

B. For the case of $b > c$

The curve (2) in Fig. 5(a) shows the effective restoring force for the case of $b > c$ when a low external electric field

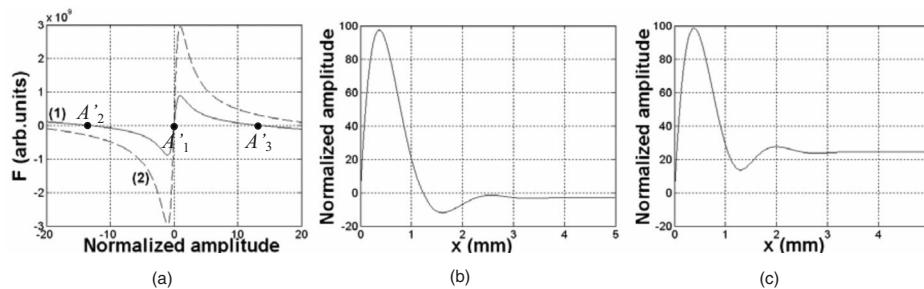


FIG. 4. (a) Effective restoring force F as a function of the normalized amplitude $A'(x)$: curves (1) and (2) correspond to $E_0 = 200$ V/cm and $E_0 = 1000$ V/cm, respectively. [(b) and (c)] Profiles of the modes corresponding to $E_0 = 200$ V/cm and $E_0 = 1000$ V/cm, respectively. The parameters b and c are $b = 1.20 \times 10^9$ m $^{-2}$ and $c = 1.21 \times 10^9$ m $^{-2}$.

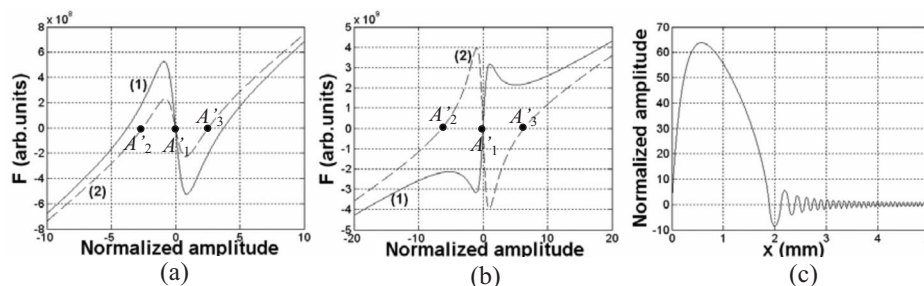


FIG. 5. (a) Effective restoring force F as a function of the normalized amplitude $A'(x)$: curves (1) and (2) correspond to $E_0=0$ V/cm and $E_0=150$ V/cm, respectively; (b) F as a function of $A'(x)$: curves (1) and (2) correspond to $E_0=1$ kV/cm and $E_0=-1$ kV/cm, respectively; (c) profile of the mode corresponding to $E_0=-1.5$ kV/cm. The parameters b and c are $b=1.23 \times 10^9$ m $^{-2}$, $c=1.21 \times 10^9$ m $^{-2}$.

$E_0 < (k_0^2 n^2 - \beta^2) / k_0^2 n^4 r_{\text{eff}}$ is applied. We can see from Fig. 5(a) that the character of the effective restoring force under a low external electric field is similar to the case of $|E_0|=0$, i.e., curve (1) as shown in Fig. 5(a). There are also three intersections $A'_{1,2,3}$ of F and $A'(x)$. $A'_1=0$ is an equilibrium position, so the oscillating can converge at 0 and the PR SW can exist steadily, but the intensity of the PR SW is still too low to have some applications; $A'_{2,3}$ are not equilibrium positions; the decaying oscillating cannot converge at the couple of nonzero values at $x \rightarrow \infty$.

The curve (1) in Fig. 5(b) shows the effective restoring force when a high external electric field $E_0 > (k_0^2 n^2 - \beta^2) / k_0^2 n^4 r_{\text{eff}}$ is applied. We can see from the curve that there is only one intersection of F and $A'(x)$: A'_1 . The position is not an equilibrium position because F always acts as a repulsive force around this position, so the PR SW cannot exist.

The curve (2) in Fig. 5(b) shows the effective restoring force when a high negative electric field $|E_0| > (k_0^2 n^2 - \beta^2) / k_0^2 n^4 r_{\text{eff}}$ is applied. We can see that there are three intersections of F and $A'(x)$: $A'_{1,2,3}$; $A(x)$ can only converge at A'_1 , which is an equilibrium position. When the value of the negative electric field is high enough, we can get the PR SW with high intensity as shown in Fig. 5(c). That provides a possibility to generate a practical PR SW with high intensity in the photovoltaic crystal under the circumstance of $b > c$.

VI. INFLUENCE OF DARK INTENSITY AND BACKGROUND ILLUMINATION

The ratio between the SW's intensity and the dark intensity can also affect the PR SW dramatically. One can see

from Fig. 6 that the spatial frequency of the SW increases with the decrease of I/I_d ; the original steep decay is replaced by a flatter one and the oscillating tail emerges in the volume of the PRC along with the decrease of I/I_d .

When a uniform background illumination I_b is applied, then Eq. (11) can be modified as

$$\frac{d^2 A'(x)}{dx^2} + \gamma \frac{A'^2(x)}{A'^2(x) + I'_b + 1} \frac{dA'(x)}{dx} - a \frac{(I'_\infty + I'_b + 1)A(x)}{A'^2(x) + I'_b + 1} - b \frac{[A'^2(x) - I'_\infty]A'(x)}{A'^2(x) + I'_b + 1} + cA'(x) = 0, \quad (20)$$

where $I'_b = I_b / I_d$ is the normalized background illumination. Equation (20) indicates that the influence of background illumination on the SW is similar to the influence of dark intensity, that is to say, background illumination is unfavorable to the formation of low-frequency modes. So if a better low-frequency mode is wanted, background illumination should be avoided.

VII. CONCLUSIONS

In summary, we studied the influence of the photovoltaic effect and the applied external electric field on the PR SW with a diffusion mechanism numerically. We provide a possible method to make the mode of the SW transform between high-frequency modes and low-frequency modes by external electric field. Some other important questions need more detailed analyses, such as the PR SW on an open-circuit condition and the stability of the PR SW. On an open-circuit condition ($J_\infty=0$), the approximate method used in a close-

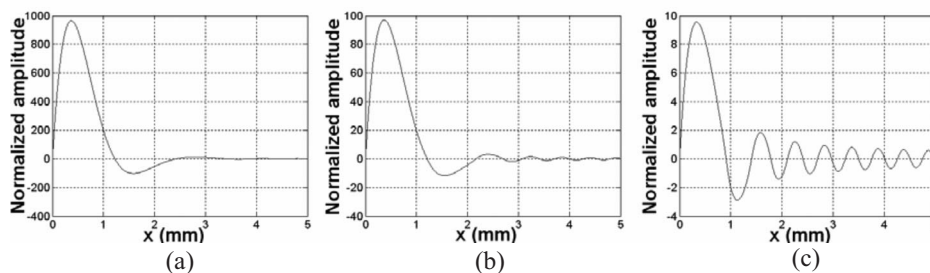


FIG. 6. Profile of the mode with a different ratio between the SW's intensity and the dark intensity: the ratio is 8.8×10^3 , 8.8×10^2 , and 8.8×10^1 for (a), (b), and (c), respectively. The parameters E_0 , b , and c are $E_0=150$ V/cm, $b=1.20 \times 10^9$ m $^{-2}$, and $c=1.21 \times 10^9$ m $^{-2}$.

circuit condition will result in the absence of external electric field E_0 in the expression of the induced space-charge field $E_{sc}(x)$, which makes the calculation of $E_{sc}(x)$ and the analysis of the SW more complex. We will study both the PR SW on open circuit and the stability of the PR SW in detail in the future.

ACKNOWLEDGMENTS

This work is supported by the National Nature Science Foundation of China under Grants No. 60208002 and No. 60678026 and Program for Changjiang Scholars and Innovative Research Team.

-
- [1] P. Yeh, *Introduction to Photorefractive Nonlinear Optics* (Wiley, New York, 1993).
- [2] Ron Daisy and Baruch Fischer, *Opt. Lett.* **17**, 847 (1992).
- [3] Ron Daisy and Baruch Fischer, *J. Opt. Soc. Am. B* **11**, 1059 (1994).
- [4] G. S. Garcia Quirino, J. J. Sanchez Mondragon, and S. Stepanov, *Phys. Rev. A* **51**, 1571 (1995).
- [5] E. Raita, A. A. Kamshilin, and T. Jaaskelainen, *J. Opt. Soc. Am. B* **15**, 2023 (1998).
- [6] I. I. Smolyaninov, C. H. Lee, and C. C. Davis, *Phys. Rev. Lett.* **83**, 2429 (1999).
- [7] T. H. Zhang, J. Yang, H. Z. Kang, L. Feng, J. J. Xu, C. P. Zhang, X. K. Ren, B. H. Wang, Y. Z. Lu, F. Jia, and W. W. Shao, *Phys. Rev. B* **73**, 153402 (2006).
- [8] A. W. Snyder and F. Ladouceur, *Opt. Photonics News* **10**, 35 (1999).
- [9] T. H. Zhang, X. K. Ren, B. H. Wang, Z. J. Hu, W. W. Shao, J. Yang, H. Z. Kang, D. P. Yang, Y. Z. Lu, L. Feng, W. J. Wang, and J. J. Xu, *J. Mod. Opt.* **54**, 1445 (2007).
- [10] M. Cronin-Golomb, *Opt. Lett.* **20**, 2075 (1995).
- [11] Igor I. Smolyaninov and C. Davis, *Opt. Lett.* **24**, 1367 (1999).
- [12] V. A. Aleshkevich, V. A. Vysloukh, and A. A. Egorov, *Proc. SPIE* **3404**, 384 (1997).
- [13] V. Aleshkevich, Y. Kartashov, A. Egorov, and V. Vysloukh, *Phys. Rev. E* **64**, 056610 (2001).
- [14] E. Alvarado-Méndez, J. A. Andrade-Lucio, R. Rojas-Laguna, J. M. Estudillo-Ayala, J. G. Aviña-Cervantes, O. G. Ibarra-Manzano, and V. Vysloukh, *Rev. Mex. Fis.* **50**, 478 (2004).
- [15] T. H. Zhang, Y. Z. Lu, H. Z. Kang, D. P. Yang, J. Y. Zheng, Z. Y. Fang, C. B. Lou, J. Yang, H. Z. Yang, and M. R. Yin, *Acta Phys. Sin.* **54**, 4688 (2005).
- [16] T. H. Zhang, H. Z. Kang, Y. Z. Lu, D. P. Yang, J. Y. Zheng, C. B. Lou, J. Yang, H. Z. Yang, and M. R. Yin, *OSA Trends Opt. Photonics Ser.* **11**, 412 (2005).
- [17] D. N. Christodoulides and M. I. Carvalho, *J. Opt. Soc. Am. B* **12**, 1628 (1995).
- [18] Jaw-Jueh Liu, Partha P. Banerjee, and Q. Wang Song, *J. Opt. Soc. Am. B* **11**, 1688 (1994).